Cross-Flow Ultrafiltration of Micellar Surfactant Solutions

John H. Markels, Scott Lynn, and Clayton J. Radke
Dept. of Chemical Engineering, University of California, Berkeley, CA 94720

A steady-state fouling-resistance and osmotic-pressure model is used to predict flux in the laminar, cross-flow ultrafiltration of micellar cetyl (=hexadecyl)pyridinium chloride (CPC) solutions at 0.01-M NaCl background electrolyte. The model assumes a constant overall hydraulic resistance including the effect of surfactant fouling and native membrane resistance. Measurements of osmotic pressures of CPC solutions at 0.01-M NaCl as a function of surfactant concentration describe the effect of concentration polarization on permeate flux. Two types of asymmetric polyethersulfone membranes are used: 5,000 molecular weight cutoff (MWCO) membranes that allow partial monomer permeation, but quantitatively reject all micelles; 50,000 MWCO membranes that allow some micelle permeation. For the former, the intrinsic rejection coefficient for monomer, measured separately, is sufficient to describe surfactant rejection, without adjustable parameters. Predictions of the volumetric flux of the permeate, including the value of the limiting flux, agree well with the experimental results over the entire range of pressure drop, axial velocity, and bulk surfactant concentration. For the 50,000 MWCO membranes the data are described using a best-fit value of the overall surfactant rejection coefficient. For the first time, unusual behavior is observed experimentally in which the flux levels off with increasing pressure drop across the membrane, only to increase sharply again at higher applied pressure drop. Both effects are in accord with the proposed model. No gel layer need be postulated to explain the flux behavior of either membrane type.

Introduction

Because of their unique aggregation and solubilization properties, surfactant micelles have been widely proposed as agents for the removal of organic contaminants from water (Leung, 1979; Dunn et al., 1985; Bhat et al., 1987; Gibbs et al., 1987; Smith et al., 1987) and from soil (Ellis et al., 1985; Gannon et al., 1989; McDermott et al., 1989; Wilson et al., 1989). An ultrafiltration (UF) step can concentrate micellar aggregates and their associated solutes, and can liberate clean water in the permeate (Leung, 1979). Industrial ultrafilters are designed to operate in cross-flow because the imposed axial velocity decreases the solute concentration at the membrane surface (reduces concentration polarization), thereby increasing solvent flux through the membrane (Cheryan, 1986).

In ultrafiltration, design and scale-up are typically achieved empirically, based on laboratory or pilot-scale results. To avoid the expense of this approach and to create an efficient design procedure, a practical and reliable model for the prediction of permeate flux in cross-flow UF is required that is based on the relevant physical phenomena. Currently, such a model is unavailable for the ultrafiltration of micellar surfactant systems because the mechanisms of flux reduction associated with concentration polarization and fouling are not well understood (Dunn et al., 1987). Here, we combine results on the intrinsic rejection behavior of membranes (Markels et al., 1994), surfactant osmotic pressure (Markels, 1993, chap. 3), and membrane fouling (Markels, 1993, chap. 4). The resultant osmotic-pressure and fouling-resistance model is used to predict flux in the cross-flow ultrafiltration of micellar cetyl(=hexadecyl)pyridinium chloride (CPC) solutions by asymmetric, polyethersulfone (PES) ultrafiltration membranes.

Correspondence concerning this article should be addressed to C. J. Radke.

J. H. Markels is currently at Merck & Co., Inc., P.O. Box 4, WP28-70, West Point, PA 19486.

Theory

Steady, cross-flow micellar ultrafiltration is illustrated in Figure 1. For the highly rejecting membranes considered here, the permeate volumetric flux, V_y, can be written as

$$V_y = \frac{\Delta P - \Delta \Pi}{R_m + R_f + R_p} \tag{1}$$

where $\Delta P = P_f - P_p$ is the applied pressure difference across the membrane (between the feed and the permeate), $\Delta \Pi = \Pi_m - \Pi_p$ is the osmotic pressure difference across the membrane (between the membrane surface and the permeate), and R_m is the membrane nascent hydraulic resistance. Other resistances included are R_f, the hydraulic resistance due to fouling on or within the membrane, and R_p, any resistance due to the concentration-polarization layer, or "gel layer" (Porter, 1972). The osmotic pressure difference across the membrane results from the difference in surfactant concentration between the membrane surface and the permeate. This concentration difference creates a driving force for solvent flow from the permeate side of the membrane to the retentate side, and thereby reduces the net pressure driving force for permeate flow in the opposite direction.

The integrated result of a differential solution mass balance yields the familiar relationship for the transmembrane velocity (volumetric flux),

$$V_y = k \ln \frac{(C_m - C_p)}{(C_b - C_p)} \tag{2}$$

where C_m, C_p, and C_b are the total surfactant concentrations, expressed as monomer, at the membrane surface, in the permeate, and in bulk solution above the membrane, respectively (Belfort and Nagata, 1985). The channel-length averaged mass-transfer coefficient, k, can be approximated by the standard Deissler correlation for laminar cross-flow UF (Porter, 1972; Nabetani et al., 1990), as

$$Sh = \left(\frac{kD_h}{D}\right) = 1.62\left[Pe\left(\frac{D_h}{L}\right)\right]^{1/3}, \tag{3}$$

where D is the diffusivity of the rejected solute, L and D_h are the length and hydraulic diameter, respectively, of the retentate cross-flow channel, Sh and $Pe = V_x L/D$ are the Sherwood and Peclet numbers, respectively, and V_x is the average axial velocity. For surfactant systems containing micellar aggregates in equilibrium with monomers, D is defined to account for diffusion of total surfactant, including both micelles and monomers (Weinheimer et al., 1981; Evans et al., 1983) and is taken as 1.8×10^{-6} cm^2/s for CPC.

A key assumption in the proposed model is that the membrane is differential: the cross-flow velocity is high enough relative to the permeate volumetric flux that there are no variations in concentration and axial or transmembrane velocity in the direction of flow along the membrane. This assumption reduces the model to the set of algebraic equations given earlier. An extended differential model, including axial variations in velocity and concentration is readily formulated. A simple ordering analysis performed on that extended model demonstrates that the criterion for a differential ultrafilter is $hV_x(R_m + R_f + R_p)/L(\Delta P - \Delta \Pi) \gg 1$, where h is the height of the cross-flow channel (Markels, 1993, append. 6D). In our experiments this ratio is typically of order 10 to 50, and the criterion is well met.

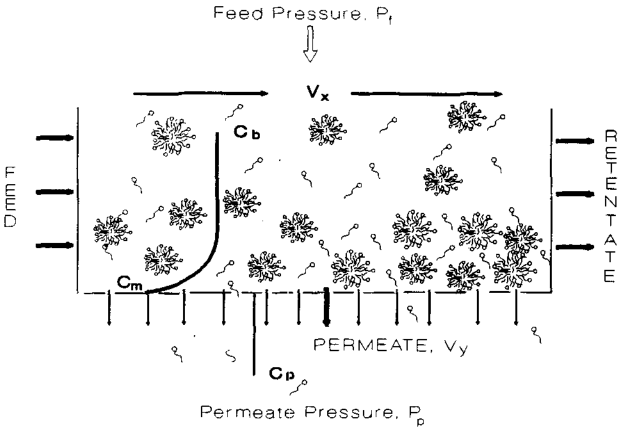

Figure 1. Differential cross-flow micellar ultrafiltration.

The UF experiments discussed in this work were performed using aqueous CPC solutions in 0.01-M NaCl. Because the membranes used are permeable to sodium and chloride ions, the permeate solution is expected to be at approximately 0.01 M NaCl. The appropriate osmotic pressure for use in Eq. 1 is the osmotic pressure relative to a solvent of 0.01 M NaCl. Recently, such relative osmotic pressures of CPC solutions in 0.01 M NaCl were measured by membrane osmometry using a nanofiltration membrane as the semipermeable barrier (Markels, 1993, chap. 3). The experimental osmometer employed is similar in design to that used by Vilker et al. (1984). The cell consists of two compartments, one charged with aqueous solvent (0.01-M NaCl) and the other with the surfactant solution (CPC + 0.01-M NaCl), separated by the semipermeable membrane. Each chamber leads into a volumetric tube, made from a graduated pipette (2.3-mm-ID of volume 1 cm^3 with 0.02 cm^3 graduations). Using regulated air, the solution-side pressure is increased manually as necessary to keep the liquid level at its original position. This is done in response to increases in the level in the solution-side pipette due to osmotic solvent transport. Eventually, the two levels remain equal and constant for several hours, and the corresponding steady applied pressure is the experimental osmotic pressure. The practice of applying pressure to the solution to prevent osmosis has major benefits. Because the initial and final liquid levels are equal, net solvent transport across the membrane during the experiment is zero. Therefore, the surfactant concentration in the solution chamber remains constant throughout the experiment, eliminating the difficulty of determining concentration after equilibrium is achieved. In addition, since there is no net solvent transport, the equilibration time using this device is much shorter than for a traditional osmometer.

The experimental results for the osmotic pressure of CPC solutions in 0.01 M NaCl are shown in Figure 2. An empirical fit to those data gives the relative osmotic pressure in units of kPa as

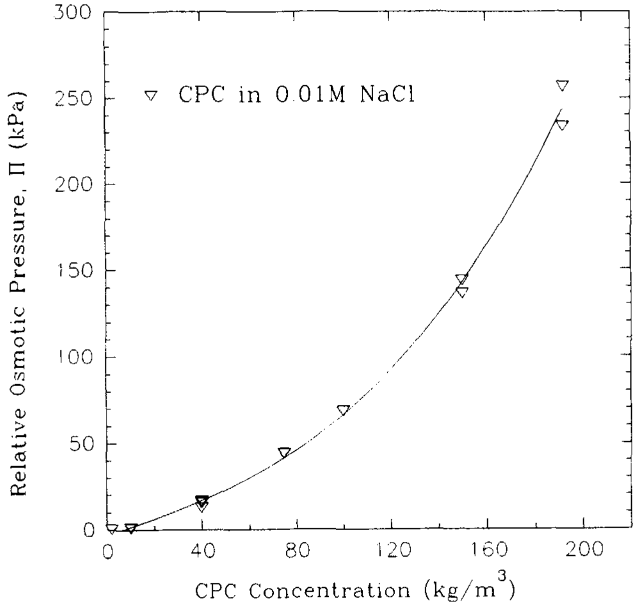

Figure 2. Experimental osmotic pressures of CPC solutions in 0.01-M NaCl.

The solid line corresponds to Eq. 4.

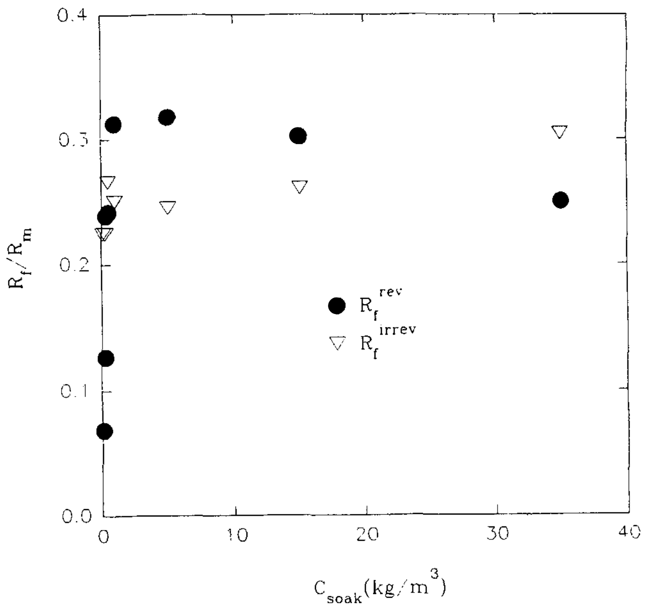

Figure 3. Normalized reversible (●) and irreversible (▽) fouling resistances of statically and dynamically fouled 50,000-MWCO UF membranes as a function of CPC concentration.

$$\Pi = 0.00366C + 0.01209C^2 - 8.0\times10^{-5}C^3 + 2.592\times10^{-7}C^4, \quad \text{for } C \leq 250\,\text{kg/m}^3, \quad (4)$$

where C is the total surfactant concentration in kg/m^3. The relative osmotic pressure at 180 kg/m^3, for example, is approximately 210 kPa (30 psi). Since the applied transmembrane pressure drop in UF is typically 210–1,030 kPa (30–150 psi), osmotic pressures of this magnitude are clearly important (Cheryan, 1986).

The surfactant concentration in the permeate in Eq. 2 is commonly related to the concentration at the membrane surface by an intrinsic membrane rejection coefficient, which is typically constant (Kedem and Katchalsky, 1958; Robertson and Zydney, 1987; Opong and Zydney, 1991). In surfactant solutions, where surfactant monomer at the critical micelle concentration (cmc) is in equilibrium with a size distribution of micelles, the situation is more complex. By measuring the permeate surfactant concentration as a function of time from an unstirred, batch UF cell operated at constant flux, we find that, for membranes that completely reject micelles and partially reject monomer (termed "Type I" membranes), the concentration of surfactant in the permeate is proportional to the monomer concentration at the membrane surface rather than the total surfactant concentration (Markels et al., 1994). Therefore, for Type I membranes, an intrinsic monomer rejection coefficient is defined as

$$R_1 = 1 - \frac{C_p}{C_m^1}, \quad (5)$$

where C_m^1 is the monomer concentration at the membrane surface. Asymmetric, polyethersulfone NOVA 5,000 molecular-weight-cutoff (MWCO) membranes are of Type I. They reject micelles quantitatively and exhibit a monomer rejection coefficient of 0.80 (Markels et al., 1994). In most practical circumstances, where the surfactant concentration at the membrane surface is large relative to the critical micelle concentration (such as greater than ten times the cmc), total surfactant rejection is nearly complete since monomers account for only a small fraction of the total surfactant at the membrane surface. In the same study, Markels et al. (1994) showed that NOVA 50,000 MWCO membranes are of Type II in that they exhibit micelle leakage through some pores. Here, surfactant rejection by these Type II membranes is successfully described by an overall rejection coefficient, defined as $R \equiv 1 - C_p/C_m$.

An unstirred batch cell was also used to study the effects of fouling on membrane resistance in the ultrafiltration of monomeric and micellar surfactant solutions (Markels, 1993, chap. 4). Fouling by the cationic surfactant cetylpyridinium chloride of oppositely charged, hydrophobic, polyethersulfone membranes exhibits a reversible component due to surfactant adsorption and an irreversible component associated with the blockage of pores. As seen in the typical data graphed in Figure 3 for a 50,000 MWCO PES membrane, both types of fouling cause a significant increase in the nascent membrane resistance. Further, each fouling resistance is essentially constant for surfactant concentrations at the membrane surface in excess of the cmc, indicating that both fouling mechanisms are controlled by surfactant monomers (which have a nearly constant concentration above the cmc). Therefore, we take $R_f = R_f^{\text{rev}} + R_f^{\text{irrev}}$ as a constant in the proposed flux model.

As detailed in the thesis of Markels (1993, chap. 4), static (zero flux) equilibration of a surfactant solution with the membrane sieving surface and subsequent water filtration was used to determine any effects of reversible adsorption. The mass of surfactant adsorbed and the flow resistance proved

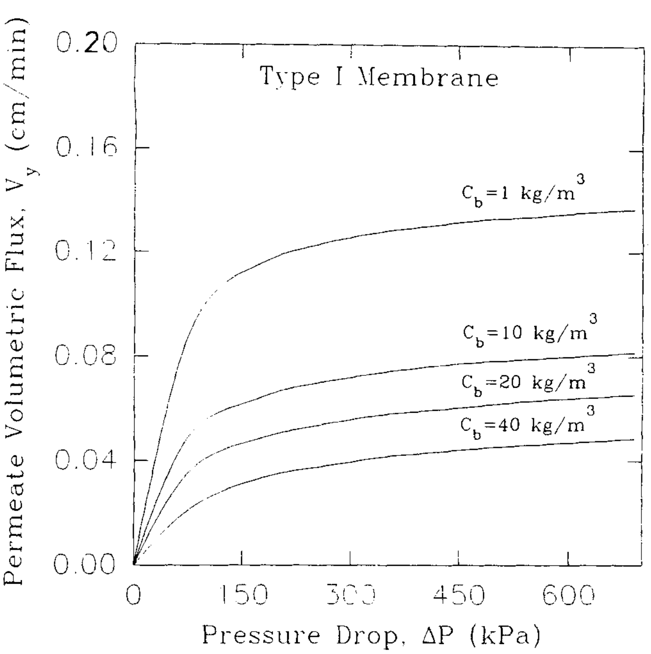

Figure 4. Model results for permeate flux in the ultrafiltration of CPC through a Type I membrane.

$V_x = 23.1$ cm/s; $R_1 = 0.80$; $R_m + R_f = 3.1 \times 10^7$ kPa·s/m; $C_{cmc} = 0.3$ kg/m^3.

to be independent of the equilibration concentration above the cmc for both 5,000 molecular weight cutoff (MWCO) membranes (which reject micelles completely) and 50,000 MWCO membranes (which do not). As reported in Figure 3, additional irreversible fouling, consistent with pore blockage at the membrane surface, was determined to occur in the presence of an applied pressure gradient. The hydraulic resistance caused by this blockage was also found to be independent of the total CPC concentration above the cmc.

In the ultrafiltration of macrosolutes, the thermodynamic reduction of the applied driving force due to the osmotic pressure gradient has in the past generally been considered to be unimportant, that is, $\Delta\Pi \sim 0$ (Trettin and Doshi, 1980, 1981; Chudacek and Fane, 1984; Wijmans et al., 1984), except perhaps at very short times after pressure is first applied (Bhattacharjee and Bhattacharya, 1992). Rather, the formation of a gel layer was considered the predominant transmembrane flux-reduction mechanism. Using an unstirred batch cell at constant driving force, however, Markels (1993, chap. 5) has recently demonstrated for CPC ultrafiltration that all of the observed reduction in flux is well accounted for solely by osmotic backpressure and solute-adsorption fouling, without assuming a gel-layer resistance. Hence, $R_p = 0$ in Eq. 1, and we recover the osmotic-pressure and fouling-resistance model used successfully by Nabetani et al. (1990) to predict flux in the ultrafiltration of ovalbumin solutions. Here it is used to model the ultrafiltration of micellar CPC solutions.

Given the cross-flow velocity, the applied transmembrane pressure drop, the CPC feed concentration, and the system geometry, Eqs. 1 through 5 are solved iteratively (Markels, 1993, append. 6A). There are no adjustable parameters since R_m, R_f, R_1, and $\Pi(C)$ are all measured independently of the cross-flow experiment, and all physical constants are known. Typical model results for Type I membranes are illustrated in Figure 4 (using the geometry of the experimental system described in the Experimental section), which plots the permeate superficial velocity (volumetric flux) as a function of the applied pressure drop for several values of the bulk feed surfactant concentration. The critical micelle concentration for CPC is $C_{cmc} = 0.3$ kg/m^3 (Rosen, 1978; this value was verified in our laboratory and does not vary appreciably with added NaCl concentration up to 0.5 M). The permeate velocity is lower for higher bulk surfactant concentrations because of the higher osmotic backpressure. The model predicts a limiting flux, that is, a flux that is independent of the applied pressure difference, similar to that predicted by the gel-polarization model (Blatt et al., 1970; Porter, 1972). Permeate concentration for a Type I membrane is limited by the monomer concentration at the membrane surface, C_m^1. This means that the total surfactant concentration at the membrane, C_m, does not reach a constant value as the transmembrane pressure drop is increased. Rather, since C_p is fixed at the value mandated in Eq. 5, C_m always increases with increasing ΔP. The osmotic backpressure increases in turn, giving the limiting flux behavior observed.

Conversely, for the more leaky Type II membrane, the permeate concentration increases with increasing ΔP as C_m increases due to increased micelle permeation. Theoretically, C_m can reach a constant value characterized by equal permeate and bulk surfactant concentrations. This is clearly an undesirable operating condition, however, since the solute concentration in the permeate has not been reduced relative to the feed. As pressure is increased beyond this point, the net driving force increases because $\Delta\Pi$ is constant (C_m is constant) and the flux rise resumes. The concentration polarization layer has no effect on flux in the model because no gel-layer resistance is present. This behavior is illustrated in Figure 5 for a Type II membrane, which shows both the permeate volumetric flux and the concentration at the membrane surface as functions of the transmembrane pressure drop for several values of the overall rejection coefficient, R. In the two cases illustrated in Figure 5a, where the flux first levels off and then increases again ($R = 0.9944$ and $R = 0.995$), the surfactant concentration at the membrane surface attains a constant value (Figure 5b). At the higher values of R where C_m continues to increase with increasing ΔP, the flux becomes nearly constant as the pressure difference is increased because C_m and the osmotic backpressure continue to build. In both Figures 5a and 5b it appears that the behaviors for $R = 0.995$ and $R = 0.997$ are fundamentally different, but they are not. In Figure 5a, for example, V_y for $R = 0.997$ will eventually rise sharply again in the same way that it does for smaller R. Because the rejection is larger, more pressure drop is required for C_p to reach C_b; in this case, more than 650 kPa. For $R = 1$, though, $C_p = 0$ and C_m rises without bound.

Experimental

CPC was used as received from Chemie AG, Switzerland (purity > 98%). Surfactant solutions were prepared by dissolving CPC in distilled and deionized water at 0.01 M NaCl that had been ultrafiltered through a 5,000 MWCO membrane to remove any particulates. CPC concentrations were

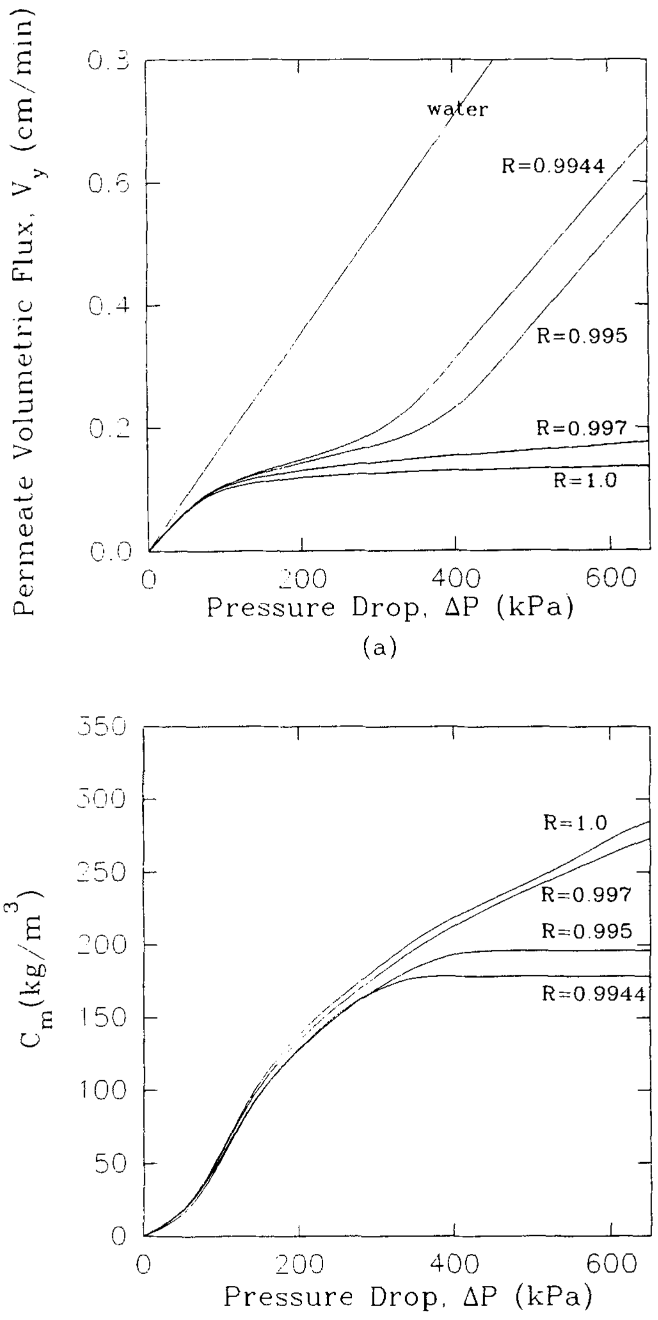

(a)

(b)

Figure 5. Model results for (a) permeate flux and (b) CPC concentration at the membrane surface in the ultrafiltration of CPC through a Type II membrane.

$C_b = 1.0$ kg/m^3; $V_x = 10.8$ cm/s; $R_m + R_f = 4.5 \times 10^5$ kPa·s/m; $C_{cmc} = 0.3$ kg/m^3.

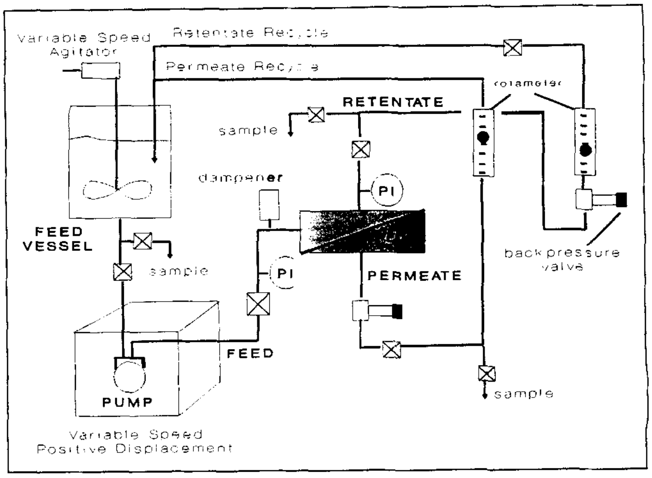

Figure 6. Cross-flow ultrafiltration experimental apparatus.

measured by UV spectrophotometry at 254 nm. A Filtron minisette laboratory cross-flow UF cell with 140-cm^2 membrane area was used in the flow apparatus illustrated in Figure 6. Both the permeate and retentate streams were recycled to the well-stirred 2,000-cm^3 feed tank to allow steady-state operation. Fluid temperature was 25 ± 3°C. Flow rates were measured using rotameters (Gilmont Instruments: permeate flow error [Type I membranes] = ±1.6 cm^3/min, permeate flow error [Type II membranes] = ±0.5 cm^3/min; retentate flow error = ±4 cm^3/min). Typical Reynolds numbers, based on the retentate channel hydraulic diameter, were of order unity. A Procon positive displacement, vane-feed pump, coupled with a needle backpressure valve on the retentate, allowed the cross-flow velocity and the transmembrane pressure drop to be varied independently. A closed-pipe pressure dampener (80 cm^3 volume) was installed at the pump outlet to minimize feed pressure variations caused by pump oscillations. A two-blade glass agitator, controlled by a Stir-Pak controller, was used at > 1,300 rpm to maintain a homogenous, bubble-free feed solution. The feed and permeate pressures were measured using WIKA pressure gauges (± 1.4 kPa).

Filtron PES 5,000 and 50,000 WMCO membranes were used. These asymmetric membranes are hydrophobic and have a slight negative charge. Average pore radii are approximately 3–10 Å and 30–60 Å for the two types, respectively (Filtron, Danvers, MA). The geometry of the membrane packet is illustrated in Figure 7. An open-channel retentate spacer was used to avoid promotion of turbulence and to allow the use of standard mass-transfer correlations. The packet contains two membranes, each with a retentate channel on

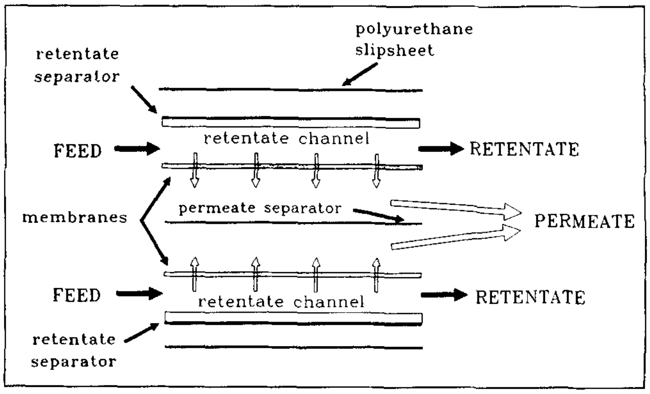

Figure 7. Flow configuration of membrane packets used in ultrafiltration experiments.

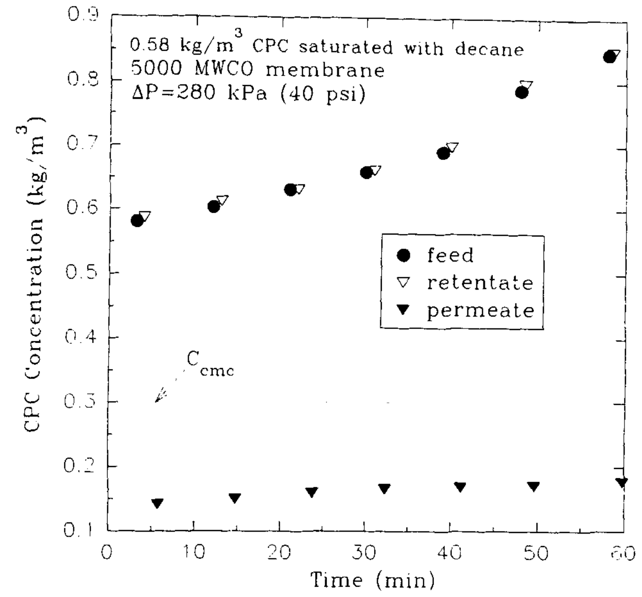

Figure 8. Transient cross-flow ultrafiltration of 0.58-kg/m^3 CPC saturated with decane.

Experimental results using a 5,000-MWCO membrane and retentate recycle.

the outside and a permeate channel on the inside. The height and width of the retentate channel are 0.0305 and 10.16 cm, respectively, and the cross-flow length, L, is 10.0 cm. Glycerin, used by the manufacturer as a membrane wetting agent, was removed from new membranes by prefiltering 0.1 m^3 of pure water.

The experiments were performed using a single membrane of each type (5,000 and 50,000 MWCO). The effect of membrane variability on the results is not addressed specifically in this study. However, experience indicates that lot-to-lot variability in membrane performance can be significant (Cheryan, 1986; Markels et al., 1994). As discussed in the Results section, this is especially true for Type II membranes, for which the model results are sensitive to variations in the intrinsic rejection characteristics.

Before performing the flux experiments, a series of tests was run to demonstrate the feasibility of cross-flow micellar ultrafiltration for micelle rejection. The retentate stream was recycled to the feed vessel as in Figure 6, but the permeate stream was not. Typical results are illustrated in Figure 8 for filtration of a CPC solution through the Type I membrane at about twice the cmc and saturated with decane. Decane was added to simulate a practical micellar ultrafiltration application, in which the solubilizing properties of the micelles and their rejection by the membrane are utilized to remove the organic contaminant from water. Micelle rejection during ultrafiltration is indicated by the increase in the retentate surfactant concentration as a function of time and by the low permeate surfactant concentration, below the cmc. Reduction in the organic concentration across the membrane associated with micelle rejection was confirmed by measured permeate organic concentrations approximately 1,000 times lower than the retentate organic concentration. Details of the decane concentration determinations by flame-ionization gas chromatography are available elsewhere (Markels, 1993, append. 6B).

Notice that the permeate concentration remains essentially constant over the course of the experiment. This is consistent with results using an unstirred batch cell for UF through a Type I (5,000 MWCO) membrane, where the permeate surfactant concentration depends only on the monomer concentration at the membrane surface, in this case the cmc (Markels et al., 1994). The results also indicate, by the nearly equal values of the feed and retentate surfactant concentrations, that the ultrafilter behaves as a differential device, as justified earlier.

Total fouling resistance was measured by first filtering 0.1 kg/m^3 CPC through the membrane for 5 h. The surfactant concentration at the membrane surface is greater than the critical micelle concentration, and any irreversible fouling due to pore blockage occurs during this period (Markels, 1993, chap. 4). The membrane was then soaked in 1.0 kg/m^3 CPC for 24 h. After rinsing the membrane to remove labile surfactant, permeate flux was remeasured with pure water at 210 kPa (30 psi). The initial value of flux was used to calculate the value of $R_m + R_f$ used in the flux model (Markels, 1993, chap. 4). The initial value is used because the reversibly adsorbed surfactant slowly desorbs during the resistance measurement with pure water. After each cross-flow experiment, the membrane resistance was remeasured. No change from the initial value was observed.

To perform the actual cross-flow experiments, a CPC solution at a desired bulk concentration in 0.01-M NaCl was added to the feed tank. The applied pressure and cross-flow velocity were set at the desired values by adjusting a backpressure valve on the retentate line and the pump speed, respectively. The system was allowed to reach steady state (less than 5 min), and permeate and retentate flow rate readings were taken from the rotameters. The pump speed and backpressure were then adjusted to give a new value of the pressure drop at the same cross-flow velocity. When enough readings at that value of V_x had been obtained, the procedure was repeated at a new cross-flow velocity. Between experiments at different concentrations, the system and membrane were rinsed thoroughly with water. No difference was found between flux data taken with increasing or decreasing magnitudes of the applied pressure drop.

Results and Discussion

Typical results using a 5,000 MWCO (Type I) membrane for various cross-flow velocities are illustrated for bulk surfactant concentrations 4.2, 13.9 and 22.4 kg/m^3 in Figures 9, 10 and 11, respectively. The clean membrane resistance for the Type I membrane used is $R_m = 1.43 \times 10^7$ kPa·s/m (20,700 psi·s/cm). The symbols represent experimental values of the permeate volumetric flux as a function of the applied pressure difference. As the cross-flow velocity increases, the flux increases at a given ΔP because the surfactant concentration at the membrane surface, and the corresponding osmotic backpressure, are reduced. Flux generally increases with increasing applied pressure drop as well, though this effect is greatly reduced by concentration polarization, especially at large ΔP. Also apparent in the figures is that, under similar conditions, the permeate volumetric flux is progressively lower for increasing values of the bulk concentration, C_b. Solid lines show the corresponding model

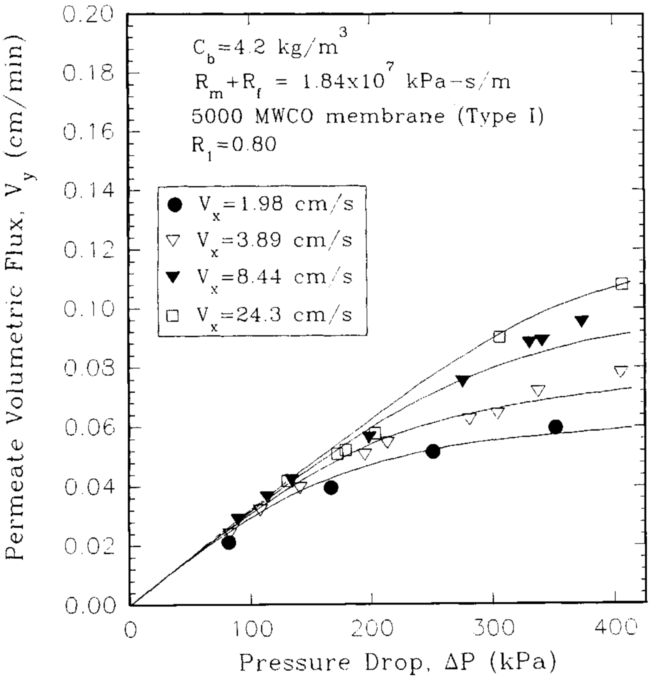

Figure 9. Steady permeate flux as a function of applied pressure drop for CPC ultrafiltration through a 5,000-MWCO membrane at C_b=4.2 kg/m^3: experiment and modeling.

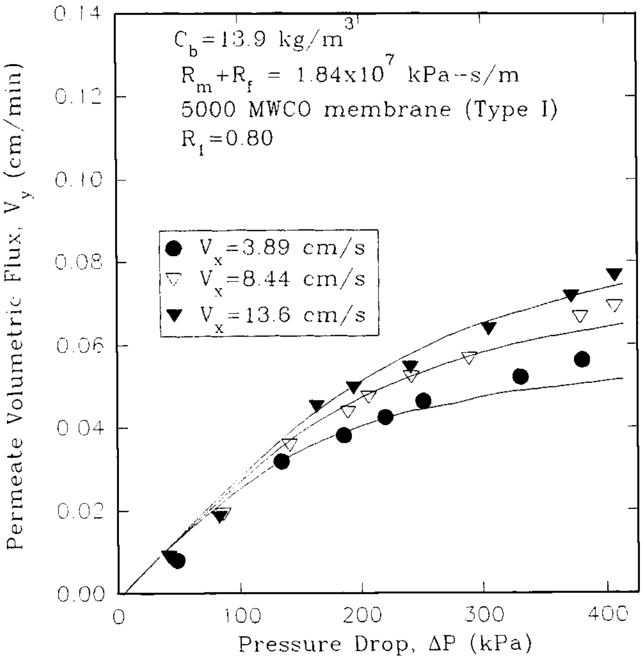

Figure 10. Steady permeate velocity as a function of applied pressure drop for CPC ultrafiltration through a 5,000-MWCO membrane at C_b= 13.9 kg/m^3: experiment and modeling.

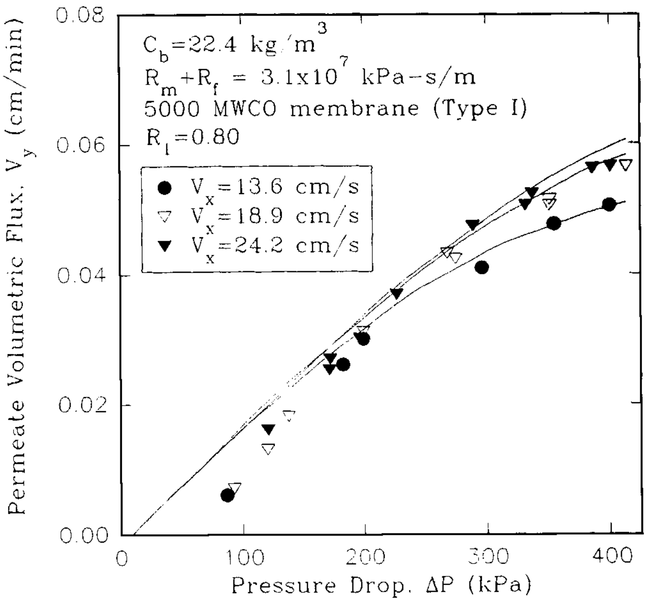

Figure 11. Steady permeate velocity as function of applied pressure drop for CPC ultrafiltration through a 5,000-MWCO membrane at C_b= 22.4 kg/m^3: experiment and modeling.

predictions using the measured values of R_1, $R_m + R_f$, and $\Pi(C)$. The model predicts the data with an accuracy of ±10% over the entire range of transmembrane pressure drop, cross-flow velocity, and bulk concentration tested using no adjustable parameters. The Deissler correlation for the laminar mass-transfer coefficient accounts for the effect of cross-flow velocity on flux. In the case of the highest cross-flow velocity, V_x = 29.6 cm/s, the Reynolds number is of order 1, clearly within the laminar regime.

Model results for the Type I membrane are insensitive to the value of the intrinsic monomer rejection coefficient, R_1. Under the highly polarized conditions studied, surfactant rejection is essentially complete, that is, monomers make up an insignificant fraction of the surfactant at the membrane surface. Systematic deviations from the predictions occur at the highest bulk concentration and lowest pressures, as seen in Figure 11. These deviations are likely due to viscous losses in the retentate channel at the highest surfactant feed concentration.

Under the conditions used, no gel-layer or polarization-layer resistance is necessary to account for the detrimental effect of concentration polarization on flux. The osmotic pressure difference across the membrane, coupled with the fouling effect of solute adsorption and pore blockage on membrane flux, are sufficient to describe the data. This is consistent with model predictions of the surfactant concentration at the membrane surface, shown in Table 1, which are in all cases below the measured turbidity limit for CPC solutions in 0.01-M NaCl at 30°C of 215 kg/m^3 (Markels, 1993, chap. 2).

Figure 12 shows the results of similar experiments using a 50,000 MWCO (Type II) PES membrane at a bulk concentration of 13.9 kg/m^3 for two different cross-flow velocities. In this case the nascent membrane resistance, R_m, is 3.1×10^5 kPa·s/m. The unusual behavior predicted by the osmotic-pressure and fouling-resistance model in Figure 5 for a Type II membrane is in fact observed. Flux is initially inhibited as concentration polarization occurs and the osmotic backpres-

Table 1. Model Predictions for the Maximum Values of the Surfactant Concentration at the Membrane Surface*

C_b (kg/m^3) Measured	V_x (cm/min) Measured	C_m (kg/m^3) Calculated
4.2	1.98	193
	3.89	176
	8.44	150
	24.3	100
13.9	3.89	199
	8.44	184
	13.6	174
22.4	13.6	143
	18.9	132
	24.2	125

*ΔP = 414 kPa (60 psi).

sure increases. Eventually, however, the concentration at the membrane surface levels off at a constant value that depends on the membrane's rejection characteristics and the bulk surfactant concentration. In these experiments, this concentration is below that at which a gel can form. The result is that as the applied pressure is increased further, the osmotic backpressure remains constant, so the net pressure driving force, and the resultant permeate flux, begin to increase again. As far as we know, this is the first time that this behavior has been observed.

The solid lines in Figure 12 show the model predictions using a one-point fit to give an overall rejection coefficient of 0.937. The excellent agreement with the data indicates that osmotic reduction of the applied transmembrane pressure drop prevails, that a steady state in the membrane surface concentration is achieved, and that there is negligible hydraulic resistance associated with the growth of the concentration polarization layer in this instance. Unfortunately, the phenomenon illustrated in Figure 10 of a rapidly increasing flux at high pressure is of little practical use because no reduction in solute concentration occurs across the membrane.

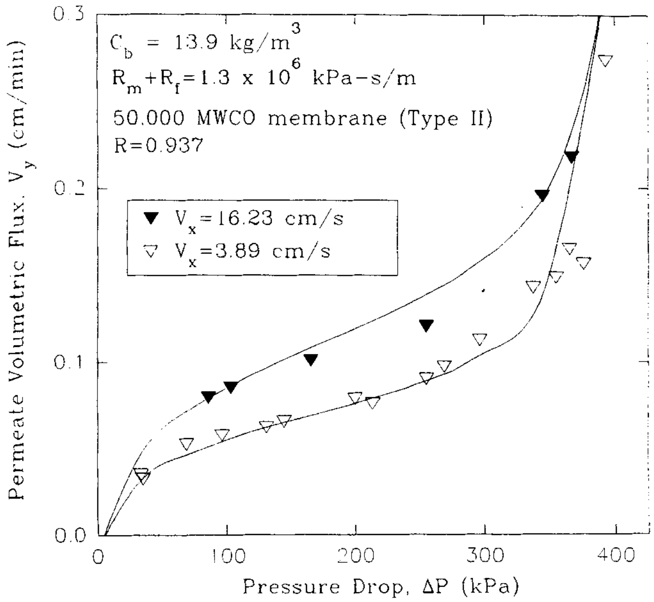

Figure 12. Steady permeate velocity as a function of applied pressure drop for CPC ultrafiltration through a 50,000-MWCO membrane at C_b = 13.9 kg/m^3: experiment and modeling.

Unlike the Type I membrane case, the model results for the Type II membrane are quite sensitive to the value of R. Small changes in R result in significant changes in C_m and, because the osmotic pressure is so sensitive to concentration, in permeate velocity.

Conclusions

A physically based transport model was developed to predict permeate flux in the steady cross-flow ultrafiltration of a micellar surfactant solution. The model utilizes measured intrinsic rejection coefficients, osmotic pressure, and membrane fouling resistance to predict the resultant steady flux at any operating condition. Agreement between model predictions and new cross-flow ultrafiltration experiments for cetylpyridinium chloride in 0.01-N NaCl clearly confirms the quantitative power of the model. The osmotic-pressure fouling-resistance model becomes a useful tool for designing industrial-scale MEUF processes (Markels et al., 1995).

For Type I membranes, which completely reject micelles, a limiting flux is caused by a reduction in the net pressure force that results from the osmotic pressure difference across the membrane. Because the surfactant rejection is nearly complete, the results are relatively insensitive to the value of the monomer rejection coefficient.

For Type II membranes, which allow some micelle permeation (50,000 MWCO), very unusual behavior is predicted by the model and observed experimentally. The flux first levels off with increasing pressure drop and then rises sharply again at still higher ΔP. These results suggest that there is no gel layer present to provide a hydraulic resistance to permeate flow and that a steady state is reached in the surfactant concentration at the membrane surface.

Acknowledgments

John Markels gratefully acknowledges Merck & Co., Inc. for financial support during an educational leave-of-absence and the North American Membrane Society for the 1992 Graduate Student Fellowship in membrane science and technology. Funding for equipment was provided by the National Institute of Environmental Health Services, under grant 3P42ES04706-0251. We also thank Filtron Technology Company, Inc., for donation of most of the membranes used.

Literature Cited

Amos, D., "Solubilization of Chlorinated Hydrocarbons in Aqueous Micellar Solutions," MS Thesis, Dept. of Chemical Engineering, Univ. of California, Berkeley (1992).

Belfort, G., and N. Nagata, "Fluid Mechanics and Crossflow Filtration: Some Thoughts," *Desalination*, **53**, 57 (1985).

Bhat, S. N., G. A. Smith, E. E. Tucker, S. D. Christian, W. Smith, and J. F. Scamehorn, "Solubilization of Cresols by *n*-Hexadecylpyridinium Chloride Micelles and Removal of Cresols from Aqueous Streams by Micellar-Enhanced Ultrafiltration," *Ind. Eng. Chem. Res.*, **26**, 1217 (1987).

Bhattacharjee, S., and P. K. Bhattacharya, "Flux Decline Behavior with Low Molecular Weight Solutes in an Unstirred Batch Cell," *J. Memb. Sci.*, **72**, 149 (1992).

Blatt, W. F., A. Dravid, A. S. Michaels, and L. M. Nelson, "Solute Polarization and Cake Formation in Membrane Ultrafiltration: Causes, Consequences, and Control Technique," *Membrane Science and Technology*, J. E. Flinn, ed., Plenum Press, New York (1970).

Cheryan, M., *Ultrafiltration Handbook*, Technomic Publishing, Lancaster, PA (1986).

Chudacek, M. W., and A. G. Fane, "The Dynamics of Polarization in Unstirred and Stirred Ultrafiltration," *J. Memb. Sci.*, **21**, 145 (1984).

Dunn, R. O., Jr., J. F. Scamehorn, and S. D. Christian, "Use of Micellar-Enhanced Ultrafiltration to Remove Dissolved Organics from Aqueous Wastes," *Sep. Sci. Tech.*, **20**(4), 257 (1985).

Dunn, R. O., Jr., J. F. Scamehorn, and S. D. Christian, "Concentration Polarization Effects in the Use of Micellar-Enhanced Ultrafiltration to Remove Dissolved Organic Pollutants from Wastewater," *Sep. Sci. Tech.*, **22**(2 & 3), 763 (1987).

Ellis, W. E., J. R. Payne, and G. D. McNabb, "Treatment of Contaminated Soils with Aqueous Surfactants," U.S. EPA Report No. EPA/600/2-85/129, PB 86-122561 (1985).

Evans, D. F., S. Mukherjee, D. J. Mitchell, and B. W. Ninham, "Surfactant Diffusion: New Results and Interpretations," *J. Colloid Interface Sci.*, **93**(1), 184 (1983).

Gannon, O. K., P. Bibring, K. Raney, J. A. Ward, and D. J. Wilson, "Soil Clean Up by *in situ* Surfactant Flushing: III. Laboratory Results," *Sep. Sci. Tech.*, **24**(14), 1073 (1989).

Gibbs, L. L., J. F. Scamehorn, and S. D. Christian, "Removal of n-Alcohols from Aqueous Streams Using Micellar-Enhanced Ultrafiltration," *J. Memb. Sci.*, **30**, 67 (1987).

Kedem, O., and A. Katchalsky, "Thermodynamic Analysis of Permeability of Biological Membranes to Non-electrolytes," *Biochim. Biophys. Acta.*, **27**, 229 (1958).

Leung, P. S., "Surfactant Micelle Enhanced Ultrafiltration," in *Ultrafiltration Membranes and Applications*, A. R. Cooper, ed., Plenum, New York, p. 415 (1979).

Markels, J. H., S. Lynn, and C. J. Radke, "Ultrafiltration of Micellar Surfactant Solutions in an Unstirred Batch Cell at Constant Flux," *J. Memb. Sci.*, **86**, 241 (1994).

Markels, J. H., S. Lynn, and C. J. Radke, "Design of Micellar-Enhanced Ultrafilters," *Ind. Eng. Chem.*, **34**, 2436 (1995).

Markels, J. H., "Batch and Continuous Ultrafiltration of Micellar Solutions: Experiment, Theory and Design," PhD Thesis, Dept. of Chemical Engineering, Univ. of California, Berkeley (1993).

McBain, J. W., and W. J. Jenkins, "The Ultrafiltration of Soap Solutions: Sodium Oleate and Potassium Laurate," *J. Amer. Chem. Soc.*, **121**, 2325 (1922).

McDermott, J. B., R. Unterman, M. Brennan, R. E. Brooks, D. P. Mobley, C. C. Schwartz, and D. D. Dietrich, "Two Strategies for PCB Soil Remediation: Biodegradation and Surfactant Extraction," *Environ. Prog.*, **8**(1), 46 (1989).

Mysels, K. J., and R. J. Otter, "Thermodynamic Aspects of Mixed Micelles—Application to an Empirically Established Equilibrium," *J. Colloid Sci.*, **16**, 474 (1961).

Nabetani, H., M. Nakajima, A. Watanabe, A. Nakao, and S. Kimura, "Effects of Osmotic Pressure and Adsorption on Ultrafiltration of Ovalbumin," *AIChE J.*, **36**(6), 907 (1990).

Opong, W. S., and A. L. Zydney, "Diffusive and Convective Transport Through Asymmetric Membranes," *AIChE J.*, **37**(10), 1497 (1991).

Porter, M. C., "Concentration Polarization with Membrane Ultrafiltration," *Ind. Eng. Chem., Prod. Res. Dev.*, **11**, 234 (1972).

Porter, M. C., in *Handbook of Separation Technologies for Chemical Engineers*, Sec. 2.1, McGraw-Hill, New York (1979).

Press, W. H., B. P. Flannery, S. A. Teukolsky, and W. J. Vetterling, *Numerical Recipes: The Art of Scientific Computing*, Cambridge Univ. Press, New York (1986).

Probstein, R. F., J. S. Shen, and W. F. Leung, "Ultrafiltration of Macromolecular Solutions at High Polarization in Laminar Channel Flow," *Desalination*, **24**, 1 (1978).

Probstein, R. F., W. F. Leung, and Y. Alliance, "Determination of Diffusivity and Gel Concentration in Laminar Ultrafiltration of Macromolecular Solutions," *J. Phys. Chem.*, **83**(9), 1228 (1979).

Robertson, B. C., "A Mass Transfer Analysis of Selective Protein Filtration with Applications to Plasma Exchange Therapy," PhD Thesis, Dept. of Chemical Engineering, Univ. of Delaware, Newark (1989).

Robertson, B. C., and A. L. Zydney, "Polarization and Adsorption Effects on Sieving in Membrane Protein Ultrafiltration," *ASAIO*, **3**, 118 (1987).

Rosen, M. J., *Surfactants and Interfacial Phenomena*, chap. 3, table 3-2, Wiley, New York (1978).

Shen, J. J. S., and R. F. Probstein, "On the Prediction of Limiting Flux in Laminar Ultrafiltration of Macromolecular Solutions," *Ind. Eng. Chem., Fundam.*, **16**, 459 (1977).

Smith, G. A., S. D. Christian, E. E. Tucker, and J. F. Scamehorn, "Equilibrium Solubilization of Benzene in Micellar Systems and Micellar-Enhanced Ultrafiltration of Aqueous Solutions of Benzene," in *Ordered Media in Chemical Separations*, W. L. Hinze and D. W. Armstrong, eds., *Amer. Chem. Soc. Ser.*, **342**, 184 (1987).

Spiegler, K. S., and O. Kedem, "Thermodynamics of Hyperfiltration (Reverse Osmosis): Criterion for Efficient Membranes," *Desalination*, **1**, 311 (1966).

Trettin, D. R., and M. R. Doshi, "Ultrafiltration in an Unstirred Batch Cell," *Ind. Eng. Chem., Fundam.*, **19**, 189 (1980).

Trettin, D. R., and M. R. Doshi, "Ultrafiltration of Colloidal Suspensions and Macromolecular Solutions in an Unstirred Batch Cell," *Ind. Eng. Chem., Fundam.*, **20**, 221 (1981).

Vilker, V. L., C. K. Colton, K. A. Smith, and D. L. Green, "The Osmotic Pressure of Concentrated Protein and Lipoprotein Solutions and its Significance to Ultrafiltration," *J. Memb. Sci.*, **20**, 63 (1984).

Weinheimer, R. M., D. F. Evans, and E. L. Cussler, "Diffusion in Surfactant Solutions," *J. Colloid Interf. Sci.*, **80**(2), 357 (1981).

Wijmans, J. G., S. Nakeo, and C. A. Smolders, "Flux Limitations in Ultrafiltration: Osmotic Pressure Model and Gel-layer Model," *J. Memb. Sci.*, **20**, 115 (1984).

Wilson, D. J., "Soil Clean Up by *in situ* Surfactant Flushing: I. Mathematical Modeling," *Sep. Sci. Tech.*, **24**(14), 1073 (1989).

Manuscript received Nov. 4, 1993, and revision received Oct. 20, 1994.